International Journal of Bifurcation and Chaos, Vol. 17, No. 5 (2007) 1623–1635

HARMONIC DISTORTION ANALYSIS BASED ON HOPF BIFURCATION THEOREM AND FAST FOURIER TRANSFORM

F. I. ROBBIO[*,†], E. E. PAOLINI[‡] and J. L. MOIOLA[*,§]
Departamento de Ingeniería Eléctrica y de Computadoras,
Universidad Nacional del Sur, (B8000CPB) Bahía Blanca, Argentina
[*]*CONICET, Argentina*
[†]*frobbio@uns.edu.ar*
[‡]*epaolini@uns.edu.ar*
[§]*jmoiola@uns.edu.ar*

G. CHEN
Department of Electronic Engineering,
City University of Hong Kong, Hong Kong SAR, P. R. China
gchen@ee.cityu.edu.hk

Received April 6, 2006; Revised May 10, 2006

A frequency domain method is used to estimate the harmonic contents of a smooth oscillation arising from the Hopf bifurcation mechanism. The harmonic contents up to the eighth-order are well estimated, which agree with the results obtained from a completely different approach that measures the frequency content of a signal by using digital signal processing techniques such as the Fast Fourier Transform (FFT). The accuracy of the approximation is evaluated by computing the Floquet multipliers of the variational system based on the fact that for periodic solutions one multiplier must be +1. The separation from this theoretical value is proportional to the error of the approximation. A limitation of the frequency domain method is encountered when being used for continuing the secondary branch of limit cycle bifurcations, such as pitchfork and period-doubling bifurcations. Two examples are shown to illustrate the main results: Colpitts' oscillator with a pitchfork bifurcation of cycles, and Chua's circuit with a period-doubling bifurcation of cycles.

Keywords: Harmonic distortion; electronic oscillator; harmonic balance; Chua's circuit; Colpitts' oscillator.

1. Introduction

Since the middle of the 20th century, the approximation of oscillatory solutions has been a challenging subject for mathematicians who have explored and refined various elaborated techniques for dealing with expressions in great accuracy not only for nearly sinusoidal but also for relaxatory orbits. Since the appearance of the intriguing results of the now well-known van der Pol oscillator, researchers have been trying to compute accurately the periodic solutions of oscillations by using different methods. In particular, frequency domain methods have a long tradition in analyzing oscillations in both autonomous and nonautonomous nonlinear systems. Starting with the simplest form, a harmonic balance method based on the classical describing function [Atherton, 1975; Mees, 1981] has been used, which is capable of showing even

the edge of chaos in some simple autonomous circuits [Genesio & Tesi, 1992]. This method uses a simple harmonic, the fundamental one, to capture the essence of an oscillation, providing some important insights for control engineers. Improvements over this approach by using subharmonic perturbations or monitoring the Floquet multipliers have been proposed [Basso *et al.*, 1997; Torrini *et al.*, 1998], which dealt with some bifurcations of limit cycles but still simply utilizing only one harmonic (plus some bias or a DC component). More elaborated expansions can be found in [Qiu & Filanovsky, 1987; Buonomo, 1998a, 1998b], and in their bibliographic lists.

With the only exception of relaxatory oscillators, such as the classical van der Pol oscillator working in the limit of large values of its bifurcation parameter, many electronic oscillators with a nearly pure sinusoidal waveform can satisfy the Hopf bifurcation theorem. This result requires that a single pair of complex eigenvalues of the linearization around an equilibrium point cross the imaginary axis when a distinguished parameter varies, at the moment of changing the stability of the singular point. Consequently, a branch of a periodic solution starts from this critical point with a characteristic root-square law of the amplitude of the oscillation. The computation of this amplitude is not a trivial task for a general system, for which some analytic methods such as multiple scales or harmonic balance based on series expansions are often used. An introduction to these techniques can be found in [Jordan & Smith, 1994] and [Strogatz, 1994], where some of the main contributions on this topic were judiciously selected. More recently, Maggio *et al.* [1999, 2004] and Robbio *et al.* [2004b] have suggested an application of the Hopf bifurcation theorem to approximating the harmonic contents in the Colpitts oscillator. In this approach, since the technique is local, the approximation is quite good when the harmonic distortion is low, which is precisely the required condition in a good oscillator where the total harmonic distortion should be below 1%. Particularly, approximation of limit cycles using the Hopf bifurcation theorem, in conjunction with the center manifold theory and normal forms, has been introduced by Maggio *et al.* [2004]. Although it has shown a good approximation of periodic solutions for a wide range of parameters, the computation of the harmonic contents is quite involved.

Limit cycle bifurcation requires the determination of parameter values at which other secondary oscillations such as those emerging from fold, flip and Neimark–Sacker bifurcations occur smoothly. Fold bifurcation involves two branches of periodic solutions coalescing in a typical turning point. Flip bifurcation is a subharmonic oscillation (of nearly half of the fundamental frequency), which gives rise to a period-2 limit cycle while the period-1 limit cycle loses its stability (supercritical flip bifurcation). Neimark–Sacker bifurcation refers to the birth of quasi-periodic motions from a single period-1 oscillation. Flip and fold bifurcations, in the realm of nonautonomous systems, have been detected lately by using the harmonic balance method, incorporating more harmonics, in order to improve the precision of the approximation in detecting those bifurcations [Piccardi, 1994, 1996].

A dramatic improvement of the precision in detecting oscillations has been obtained recently [Bonani & Gilli, 1999] by computing up to 21 harmonics in the primary periodic branches of Chua's circuit with a smooth nonlinear term [Khibnik *et al.*, 1993]. The harmonic balance method was applied to an autonomous system by carrying out efficient computations of the Floquet multipliers, so as to determine limit cycle bifurcations, mainly folds and flips.

Other frequency-based methods have also been proposed [Buonomo & Di Bello, 1996; Buonomo, 1998a; Berns *et al.*, 2001] for computing oscillations. Buonomo and Di Bello applied classical perturbation theory to determine both frequencies and amplitudes of the harmonics based on some recurrence formulas. On the other hand, Berns *et al.* computed higher-order harmonic balance formulas from a feedback system approach, approximating the periodic branch emerging from Hopf bifurcation, and then computed the Floquet multipliers for stability analysis. The same method has been tested up to eight harmonics by Robbio *et al.* [2004a], to detect saddle-node (pitchfork), flip and Neimark–Sacker bifurcations in three-dimensional systems. The computation of the periodic branch emerging from Hopf bifurcation has been revived in Colpitts' oscillator with an exponential nonlinear term [Maggio *et al.*, 2004]. In this case, a projection technique was used for the computation of the center manifold in order to approximate the corresponding oscillation. These accurate results can be of importance in detailed harmonic distortion analysis of global and complex dynamics, which certainly add a lot to harmonic distortions but are not present in the region where local methods are useful (see the complex and global behaviors discussed by Maggio *et al.* [1999]).

In the present paper, a local expansion up to eight harmonics will be computed. The methodology can also track small deviations of the frequencies of oscillations due to parameter variation. A comparison between the predicted harmonic contents and the ones obtained by applying a digital signal processing method for calculating the discrete Fourier transform is included. In this case, the *fast Fourier transform* (FFT) technique has been chosen for comparison. In this way, a second, complementary and independent measure of the precision of the harmonic contents follows the traditional accuracy test provided by the separation from +1 of the trivial Floquet multiplier [Padín *et al.*, 2005]. Furthermore, the harmonic contents of oscillations arising from Hopf bifurcation in Chua's circuit and in a model of Colpitts' oscillator, both with polynomial nonlinearities, will be computed. One contribution is in pointing out some limitations of the frequency domain method in recovering secondary oscillations, i.e. those arising from limit cycle bifurcations of the primary branch. More precisely, it will be shown that the approximation of the primary branch of a periodic solution and the determination of the limit cycle bifurcations are in good agreement with the results provided by numerical simulations. On the other hand, it will be pointed out that this method is not able to characterize the harmonic contents of the *bifurcated* limit cycle (secondary oscillation) despite its accurate localization in the bifurcation parameter range. Furthermore, the harmonic contents of the primary branch is contrasted with the one obtained from numerical simulation based on the FFT. A comparison will be provided for the modification of the amplitude of the oscillation from Colpitts' circuit, by using Buonomo's method, harmonic balance method, and numerical simulation, respectively. These results are complementary to those on harmonic distortions studied before [Qiu & Filanovsky, 1987; Buonomo, 1998a; Padín *et al.*, 2005], where the van der Pol oscillator was used with small values of the damping parameter.

2. Smooth Oscillations

Consider the general nonlinear system

$$\begin{aligned} \dot{x} &= \mathbf{A}x + \mathbf{BD}y + \mathbf{B}[g(y;\mu) - \mathbf{D}y], \\ y &= \mathbf{C}x, \end{aligned} \tag{1}$$

where $x \in \mathbb{R}^n$, $y \in \mathbb{R}^m$, $\mathbf{A}$, $\mathbf{B}$, $\mathbf{C}$ and $\mathbf{D}$ are $n \times n$, $n \times l$, $m \times n$ and $l \times m$ matrices, respectively, $\mu \in \mathbb{R}$ is the bifurcation parameter, y is the output, $\mathbf{g}: \mathbb{R}^m \times \mathbb{R} \to \mathbb{R}^l$ is at least a C^{2q+1}-function in x and μ, in which $2q$ is the order of the harmonic balance, and the matrix $\mathbf{D}$ can be rather arbitrarily chosen.

The system may be represented in feedback form with a linear transfer matrix $\mathbf{G}(s;\mu)$ in the direct path and a memoryless nonlinear part $\mathbf{f}(\cdot;\mu)$ in the feedback path, i.e.

$$\begin{aligned} \mathbf{G}(s;\mu) &= \mathbf{C}[sI - (\mathbf{A} + \mathbf{BDC})]^{-1}\mathbf{B}, \\ u &= \mathbf{f}(e;\mu) := \mathbf{g}(y;\mu) - \mathbf{D}y, \end{aligned}$$

where $e = -y$ and s is the complex variable of the Laplace transform (Fig. 1). Equilibrium points of system (1) correspond to the solutions $\hat{e}$ of

$$\mathbf{G}(0;\mu)\mathbf{f}(\hat{e};\mu) + \hat{e} = 0.$$

The open-loop linearization matrix associated with the feedback realization is $\mathbf{G}(s;\mu)\mathbf{J}(\mu)$ where

$$\mathbf{J} = \left.\frac{\partial \mathbf{f}(e;\mu)}{\partial e}\right|_{e=\hat{e}} = D_e\mathbf{f}(\hat{e};\mu),$$

and the corresponding eigenvalues are given by the roots of the following equation:

$$\begin{aligned} h(\lambda, s;\mu) &= \det[\lambda I - \mathbf{GJ}] \\ &= \lambda^p + a_{p-1}(\cdot)\lambda^{p-1} + \cdots + a_0(\cdot) = 0, \end{aligned} \tag{2}$$

where $p = m$ and $a_i(s;\mu)$ are rational functions of s. Assuming a single root of $h(\cdot)$ at $\lambda = -1$ and replacing $s = i\omega$ in Eq. (2), a necessary condition for computing a bifurcation point (ω_0, μ_0) is obtained by solving

$$h(-1, i\omega;\mu) = (-1)^p + \sum_{k=0}^{p-1} (-1)^k a_k(i\omega;\mu) = 0,$$

for ω and μ.

If $\omega_0 = 0$, then the bifurcation condition is called *static,* and it is related to the multiplicity of the equilibrium solutions. On the other hand, if $\omega_0 \neq 0$, the bifurcation condition is known as *dynamic* or *Hopf*, provided that some additional conditions are fulfilled, and it is related to the existence of periodic solutions.

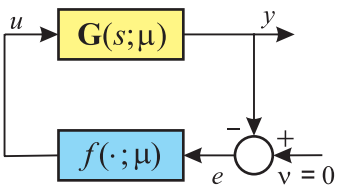

Fig. 1. Block diagram of the feedback system.

2.1. *Hopf bifurcation*

In order to analyze the Hopf bifurcation, let us split Eq. (2) with $\lambda = -1$ in real and imaginary parts, i.e.

$$\begin{aligned} F_1(\omega;\mu) &= \mathrm{Re}\{h(-1, i\omega;\mu)\} \\ &= (-1)^p + \sum_{k=0}^{p-1} (-1)^k \mathrm{Re}\{a_k(i\omega;\mu)\} = 0, \end{aligned} \tag{3}$$

$$\begin{aligned} F_2(\omega;\mu) &= \mathrm{Im}\{h(-1, i\omega;\mu)\} \\ &= \sum_{k=0}^{p-1} (-1)^k \mathrm{Im}\{a_k(i\omega;\mu)\} = 0. \end{aligned} \tag{4}$$

Then, the three basic statements of the Hopf bifurcation theorem in the frequency domain setting are:

(H1) There is only one eigenvalue of $\mathbf{G}(s;\mu)\mathbf{J}(\mu)$, denoted $\hat{\lambda}$, passing through the critical point $-1 + i0$ when ω varies in $[0, \infty)$, reflecting the change in the stability of the equilibrium solution. In addition, there is only one frequency $\omega_0 \neq 0$ satisfying Eqs. (3) and (4) for a given $\mu = \mu_0$ (avoiding a resonance condition), and $(\partial F_1/\partial\omega)(\omega_0;\mu_0)$, $(\partial F_2/\partial\omega)(\omega_0;\mu_0)$ are not simultaneously zero.

(H2) The following determinant is nonzero:

$$\det \begin{bmatrix} \dfrac{\partial F_1}{\partial \mu} & \dfrac{\partial F_2}{\partial \mu} \\ \dfrac{\partial F_1}{\partial \omega} & \dfrac{\partial F_2}{\partial \omega} \end{bmatrix}_{(\omega_0,\mu_0)} \neq 0.$$

(H3) The expression

$$\sigma_1 = -\mathrm{Re}\left\{ \frac{w^\top \mathbf{G}(i\omega_0;\mu) p_1(\omega_0;\mu)}{w^\top \mathbf{G}'(i\omega_0;\mu)\mathbf{J} v} \right\}, \tag{5}$$

called the *curvature coefficient*, does not change its sign when μ varies near μ_0.

In Eq. (5), $w^\top$ and v are respectively the left and right eigenvectors of the open-loop transfer matrix $\mathbf{G}(i\omega;\mu)\mathbf{J}(\mu)$ associated with $\hat{\lambda}$, $\mathbf{G}'(i\omega_0;\mu) = (d\mathbf{G}/ds)|_{s=i\omega_0}$, and

$$p_1(\omega;\mu) = \mathbf{Q}\mathbf{V}_{02} + \frac{1}{2}\bar{\mathbf{Q}}\mathbf{V}_{22} + \frac{1}{8}\mathbf{L}\bar{v}, \tag{6}$$

where

$$\mathbf{V}_{02} = -\frac{1}{4}\mathbf{H}(0;\mu)\mathbf{Q}\bar{v}, \tag{7}$$

$$\mathbf{V}_{22} = -\frac{1}{4}\mathbf{H}(i2\omega;\mu)\mathbf{Q}v, \tag{8}$$

with

$$\mathbf{H}(s;\mu) = [\mathbf{G}(s;\mu)\mathbf{J}(\mu) + \mathbf{I}]^{-1}\mathbf{G}(s;\mu), \tag{9}$$

in which " $\bar{\cdot}$ " denotes the complex conjugate; $\mathbf{Q}$ and $\mathbf{L}$ are $n \times l$ and $l \times m$ matrices, respectively, which contain the information of the second and third derivatives of $\mathbf{f}(e;\mu)$ evaluated at $\hat{e}$ [Mees & Chua, 1979], defined as

$$\mathbf{Q} = [Q_{jk}] = \sum_{p=1}^{m} \left.\frac{\partial^2 f_j(e)}{\partial e_p \partial e_k}\right|_{\hat{e}} v_p,$$

$$\mathbf{L} = [L_{jk}] = \sum_{p=1}^{m}\sum_{q=1}^{m} \left.\frac{\partial^3 f_j(e)}{\partial e_p \partial e_q \partial e_k}\right|_{\hat{e}} v_p v_q,$$

where $j = 1, 2, \ldots, l$; $k = 1, 2, \ldots, m$.

It is worth mentioning that Eq. (5) shows the stability of the emerging periodic solution at *criticality*: if σ_1 is negative (positive) the limit cycle is stable (unstable).

When the above conditions are fulfilled, the theorem assures the existence of oscillations in a neighborhood of the critical value of the bifurcation parameter μ_0 and allows a graphical procedure to calculate the frequency of the oscillation ω_0 and a measurement of the amplitude, noted as $\hat{\theta}$ ($\hat{\theta} \in \mathbb{R}$), by varying the parameter μ. Once the birth of a limit cycle due to a Hopf bifurcation is detected, a second-order [Mees & Chua, 1979], fourth-order [Mees, 1981], sixth- and eighth-order [Moiola & Chen, 1996], and generally a $2q$-order harmonic balance approximation (HBA) (of the periodic solution in the neighborhood of the criticality) can be obtained by using some available explicit formulas. To this end, one must solve the general equation

$$\hat{\lambda}(i\hat{\omega}_q) = -1 + \sum_{k=1}^{q} \xi_k(\hat{\omega}_q)\hat{\theta}_q^{2k}, \tag{10}$$

where $\hat{\lambda}$ is the eigenvalue associated with $\mathbf{GJ}$, whose eigenlocus crosses the real axis closest to the critical point $-1 + i0$, and $\hat{\theta}$ and $\hat{\omega}$ are approximations of the amplitude and frequency, respectively, and ξ_k are complex numbers (see the corresponding expressions in [Robbio *et al.*, 2004a] for simple 3D systems). The pair $(\hat{\omega}_q, \hat{\theta}_q)$ are obtained by means of an iterative procedure starting with ω_R, at which the frequency locus of $\hat{\lambda}$ crosses the real axis near the point $-1 + i0$, indicated as P_R in Fig. 2, in a second-order balance approximation.

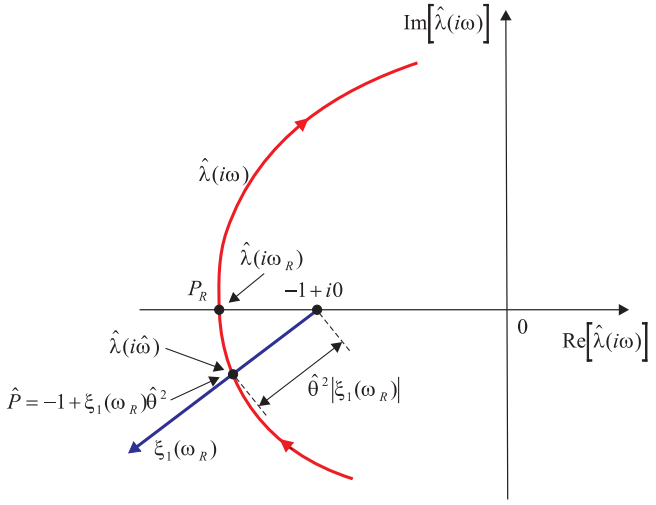

Fig. 2. Intersection between the eigenlocus $\hat{\lambda}$ and the amplitude locus $-1+\xi_1\theta^2$.

Finally, the approximation formulas for the $2q$-order HBA are

$$e(t) = \hat{e} + \mathrm{Re}\left\{\sum_{k=0}^{2q} E^k \exp(ik\hat{\omega}t)\right\}, \qquad (11)$$

where $E^0 = \hat{\theta}^2\mathbf{V}_{02}+\hat{\theta}^4\mathbf{V}_{04}+\hat{\theta}^6\mathbf{V}_{06}+\cdots+\hat{\theta}^{2q}\mathbf{V}_{0,2q}$, $E^1 = \hat{\theta}\mathbf{V}_{11}+\hat{\theta}^3\mathbf{V}_{13}+\hat{\theta}^5\mathbf{V}_{15}+\cdots+\hat{\theta}^{2q+1}\mathbf{V}_{1,2q+1}$, $E^2 = \hat{\theta}^2\mathbf{V}_{22}+\hat{\theta}^4\mathbf{V}_{24}+\hat{\theta}^6\mathbf{V}_{26}+\cdots+\hat{\theta}^{2q}\mathbf{V}_{2,2q}$ and $E^k = \hat{\theta}^k\mathbf{V}_{kk}+\hat{\theta}^{k+2}\mathbf{V}_{k,k+2}+\cdots$, are given explicitly in [Mees, 1981] and [Moiola & Chen, 1996], up to the order $2q = 8$.

To study the stability of the periodic solution, one needs to analyze the behavior of the trajectories in the neighborhood of the periodic solution. This can be done by computing the monodromy matrix $\mathbf{M}$, for which one needs to solve the variational equation

$$\dot{\mathbf{Y}}(t) = \mathbf{J}_{\mathrm{var}}(t)\mathbf{Y}(t), \quad \mathbf{Y}(0) = \mathbf{I}, \qquad (12)$$

$$\mathbf{M} = \mathbf{Y}\left(\frac{2\pi}{\hat{\omega}_q}\right), \qquad (13)$$

where $\mathbf{J}_{\mathrm{var}}$ is the Jacobian matrix of system (1) evaluated at the periodic solution.

Table 1. Multiplier crossings and cycle bifurcations.

Crossing Point	Cycle Bifurcation
$-1+i0$	Period-doubling
$1+i0$	SN, TC or PF
$\alpha \pm i\beta$ $(\alpha^2+\beta^2=1)$	Neimark–Sacker or torus

In the general case, $\mathbf{M}$ has n eigenvalues, $m_1(\mu), m_2(\mu), \ldots, m_n(\mu)$, which are known as characteristic (or Floquet) multipliers. For periodic solutions, one of them is always equal to $+1$, say $m_1(\mu)$, and the remaining $n-1$ determine the local stability of the limit cycle. Then, the periodic solution is stable if all Floquet multipliers, except the one at $+1$, are located inside the unit circle. If one or more Floquet multipliers are crossing the unit circle after a parameter variation, the periodic solution changes its stability. Generally, this situation gives rise to a bifurcation of cycles. The multiplier that crosses the unit circle is known as the *critical multiplier*, and three distinguished ways of crossing the unit circle determine three associate types of branching as shown in Table 1 and Fig. 3. The crossing of the critical multiplier at the negative real axis [Fig. 3(a)] leads to a period-doubling or flip bifurcation. When the eigenvalue crosses the unit circle at the point $+1+0i$ [Fig. 3(b)], it may indicate a saddle-node (SN), transcritical (TC), or pitchfork (PF) bifurcation, depending on the nonlinear terms and the symmetry of the system. The third type of

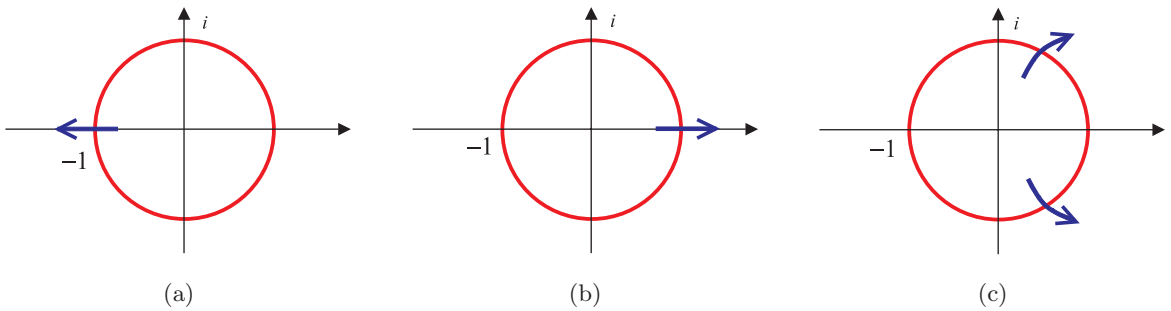

Fig. 3. Multiplier crossing conditions for bifurcations of cycles: (a) flip or period-doubling, (b) fold, transcritical or pitchfork, (c) Neimark–Sacker.

bifurcation, Neimark–Sacker or *torus* bifurcation, is characterized by a pair of complex-conjugate multipliers crossing the unit circle as shown in Fig. 3(c).

If the periodic solution is replaced by the $2q$-order HBA of the limit cycle [Eq. (11)], an approximate *monodromy matrix* $\mathbf{M}_q$ is obtained and the Jacobian $\mathbf{J}_{\rm var}(T)$ is a periodic matrix resulting from the approximation of the limit cycle $e(t)$.

It is important to mention the role that the trivial multiplier $m_1(\mu)$ plays in the measurement of the precision of the approximate solution [Guckenheimer & Meloon, 2000]: the error between the numerically computed (not real) and the approximate solution diminishes as the multiplier approaches $+1$.

2.2. *Harmonic distortion*

Harmonic distortion is an important measure of the quality of the output waveform of an oscillator since it allows to compare the amplitude of the fundamental frequency with its harmonics. In a general case, different types of distortion in elementary electric circuits can be defined by considering the nonlinear characteristic curves of the transistors. An excellent review of this topic is given by Sansen [1999].

The *harmonic distortion index* quantifies the departure of the actual solution from the ideal one. The output of an ideal oscillator is given by the component of the fundamental frequency:

$$y_1(t) = -\mathrm{Re}\{E^1 \exp(i\hat{\omega}t)\}.$$

The nonlinear terms cause variation in the operational point, $y_0(t) = -\hat{e} - E^0 = -\hat{e} - (\hat{\theta}^2\mathbf{V}_{02} + \hat{\theta}^4\mathbf{V}_{04} + \cdots + \hat{\theta}^{2q}\mathbf{V}_{0,2q})$, and in the higher-order harmonics,

$$y_k(t) = -\mathrm{Re}\{E^k \exp(ik\hat{\omega}t)\}, \quad k = 2, 3, \ldots$$

The magnitude of the harmonic influence is evaluated by *the harmonic distortion indexes*, where the kth harmonic distortion index (HD_k) is defined as the ratio of the component of frequency $k\omega$ to the one at the fundamental ω:

$$\mathrm{HD}_k(\%) = 100\frac{|E^k|}{|E^1|}, \quad k > 1.$$

From the approximate solution (11), considering up to eight harmonics results in

$$\mathrm{HD}_2 = \frac{100 \times \hat{\theta}|\mathbf{V}_{22} + \hat{\theta}^2\mathbf{V}_{24} + \hat{\theta}^4\mathbf{V}_{26} + \hat{\theta}^6\mathbf{V}_{28}|}{|\mathbf{V}_{11} + \hat{\theta}^2\mathbf{V}_{13} + \hat{\theta}^4\mathbf{V}_{15} + \hat{\theta}^6\mathbf{V}_{17} + \hat{\theta}^8\mathbf{V}_{19}|},$$

$$\mathrm{HD}_3 = \frac{100 \times \hat{\theta}^2|\mathbf{V}_{33} + \hat{\theta}^2\mathbf{V}_{35} + \hat{\theta}^4\mathbf{V}_{37}|}{|\mathbf{V}_{11} + \hat{\theta}^2\mathbf{V}_{13} + \hat{\theta}^4\mathbf{V}_{15} + \hat{\theta}^6\mathbf{V}_{17} + \hat{\theta}^8\mathbf{V}_{19}|}.$$

For small signal amplitudes, HD_2 is proportional to θ, and HD_3 to θ^2; for larger amplitudes, in general, the index loses this proportionality.

Another measure is the *total harmonic distortion* (THD), which is defined as the ratio of the higher harmonics to the one at the fundamental frequency, i.e.

$$\mathrm{THD}(\%) = 100\frac{\left(\sum_{k=2} |E^k|^2\right)^{1/2}}{|E^1|} = \sqrt{\mathrm{HD}_2^2 + \mathrm{HD}_3^2 + \cdots}.$$

It is worth mentioning that the THD is not very useful since it does not give a clear dependence on the input signal level.

3. Application Examples

In this section, the presented methodology is applied to simple flows. In all the cases, a Single-Input-Single-Output (SISO) realization is obtained since the nonlinearity involves only one variable, which results in $w^\top = v = 1$. Furthermore, a simplification of the higher-order corrections in the direction of the eigenvector v is attained.

3.1. *Colpitts' circuit*

Consider a model of the Colpitts' type of circuit described in [Buonomo & Di Bello, 1996]:

$$\begin{cases} \dot{x}_1 = \dfrac{1}{C_2}x_2, \\ \dot{x}_2 = \dfrac{1}{L}(-x_1 + x_3), \\ \dot{x}_3 = -f(x_1) - \dfrac{1}{C_1}\left[x_2 + \dfrac{1}{R}x_3\right], \end{cases} \tag{14}$$

where $f(x_1) = 1/C_1[x_1 + \mu(3x_1 + c_3x_1^3)]$ and μ is the control parameter.

It is possible to obtain an SISO feedback realization since the nonlinearity involves only one state variable, x_1. The corresponding realization of (14) is

$$\mathbf{A} = \begin{bmatrix} 0 & \dfrac{1}{C_2} & 0 \\ -\dfrac{1}{L} & 0 & \dfrac{1}{L} \\ 0 & -\dfrac{1}{C_1} & -\dfrac{1}{C_1R} \end{bmatrix}, \quad \mathbf{B} = \begin{bmatrix} 0 \\ 0 \\ 1 \end{bmatrix},$$

$$\mathbf{C} = \begin{bmatrix} 1 & 0 & 0 \end{bmatrix}, \quad D = 0,$$

$$g(x) = -\frac{1}{C_1}[x_1 + \mu(3x_1 + c_3 x_1^3)].$$

The linear transfer function $G(s;\mu)$ is $G(s;\mu) = C_1 R/\Delta(s)$, where $\Delta(s) = C_1C_2RLs^3 + C_2Ls^2 + (C_1+C_2)Rs+1$, and the nonlinear function in terms of the output $e_1 = -x_1$ is

$$f(e_1) = \frac{1}{C_1}\left[e_1 + \mu(3e_1 + c_3 e_1^3)\right].$$

The equilibrium solutions are

$$P^0 = \hat{e}_1^0 = 0, \quad P^{\pm} = \hat{e}_1^{\pm} = \pm\sqrt{-\frac{\frac{1}{R} + 1 + 3\mu}{c_3\mu}}.$$

Consider only the equilibrium point P^0. Since the system is SISO, there is only one eigenlocus, and for the values $L = 1$, $C_1 = C_2 = 2$, $R = 1/(1-2\mu)$,

$$\hat{\lambda}(s) = G(s)J = \frac{1+3\mu}{4s^3 + 2(1-2\mu)s^2 + 4s + (1-2\mu)},$$

where $J = [(1+3\mu) + 3\mu c_3 e_1^2]/C_1\big|_{P^0} = (1+3\mu)/2$.

For the Hopf bifurcation ($\omega_0 \neq 0$), the necessary condition $\hat{\lambda}(i\omega) = -1 + i0$ gives $\omega_0 = 1$, and $\mu_{\text{Hopf}} = \mu_0 = 0$. The frequency ω_R at which $\hat{\lambda}(i\omega)$ crosses the real axis satisfies

$$\operatorname{Im}\hat{\lambda}(i\omega_R) = \frac{-4\omega_R(1-\omega_R^2)(1+3\mu)i}{X(\omega_R)} = 0,$$

where $X(\omega_R) = (1-2\mu)^2(1-2\omega_R^2)^2 + 16\omega_R^2(1-\omega_R^2)^2$. It can be shown that $\omega_R = 1$. On the other hand,

$$\operatorname{Re}\hat{\lambda}(i\omega_R) = \frac{-1-3\mu}{1-2\mu}.$$

The normalized right and left eigenvectors v, $w^\top$ of the transfer function $G(i\omega_R)J$ corresponding to $\hat{\lambda}$ are $v = w^\top = 1$, and the closed-loop transfer function is $H(s) = 2/\Delta_1(s)$, where $\Delta_1(s) = 4s^3 + 2(1-2\mu)s^2 + 4s + 2 + \mu$. The complex number $p_1 = (1/8)D_3 v^2 \bar{v} = (3/8)c_3\mu$ yields $\xi_1 = -w^\top G(i\omega_R)p_1 = (3/4)c_3\mu/(1-2\mu)$. The solution of $\hat{\lambda}(i\omega_R) = -1 + \xi_1\theta^2$ gives

$$\frac{-1-3\mu}{(1-2\mu)} = -1 + \frac{3}{4}\frac{c_3\mu\theta^2}{(1-2\mu)}.$$

Solving for θ yields $\theta = \sqrt{-20/(3c_3)} \approx 1.666$ for $c_3 = -2.4$. It is important to notice that $\xi_1 = 0$ in the bifurcation condition since $\mu_0 = 0$, but this singularity disappears when μ is varied and then the method can be applied.

Computations for the fourth-, sixth- and eighth-order HBA have been implemented in a computer program. Following the Hopf bifurcation at $\mu_0 = 0$ and increasing the value of μ, a pitchfork bifurcation of cycles is detected with a continuation procedure at $\mu_{\text{PB}} = 0.2239449$. By using this method with eight harmonics, the bifurcation point is detected at the same place ($\mu_{\text{PB}\mathbf{M}_4} \approx \mu_{\text{PB}}$). As mentioned before, the deviation of the characteristic multiplier from +1 is a measure of the approximation error. In the present case (with $\mathbf{M}_4$ approximation), this deviation amounts to 3.28×10^{-6}.

Due to the nonlinearity and the equilibrium point considered, the harmonic distortion index $\text{HD}_2 = 0$. However, HD_3 is not zero, and it can be computed in terms of the parameter μ in the range $2.5 \times 10^{-3} < \mu < 0.2235$ (the range where the periodic oscillations occur). This index is contrasted with a similar one computed by numerical simulation via the FFT (Fig. 4). Also, the amplitude of the oscillation as a function of the parameter μ can be calculated by other techniques, as shown in Fig. 5, where Buonomo's formula for the output is also plotted. The results show a good agreement between the different methods.

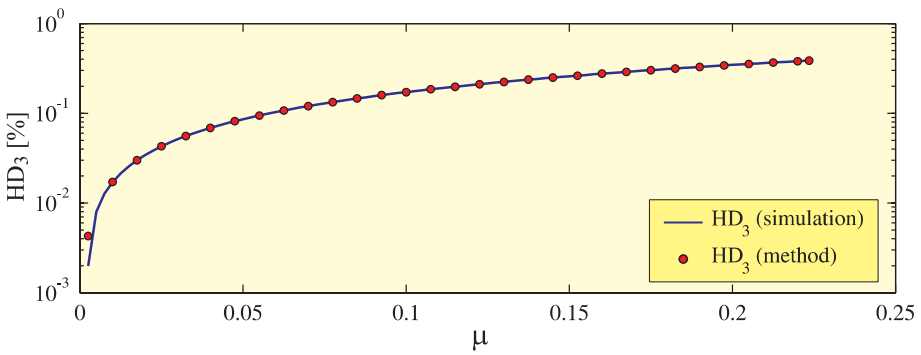

Fig. 4. Harmonic distortion index HD_3 for x_1 and $c_3 = -2.4$.

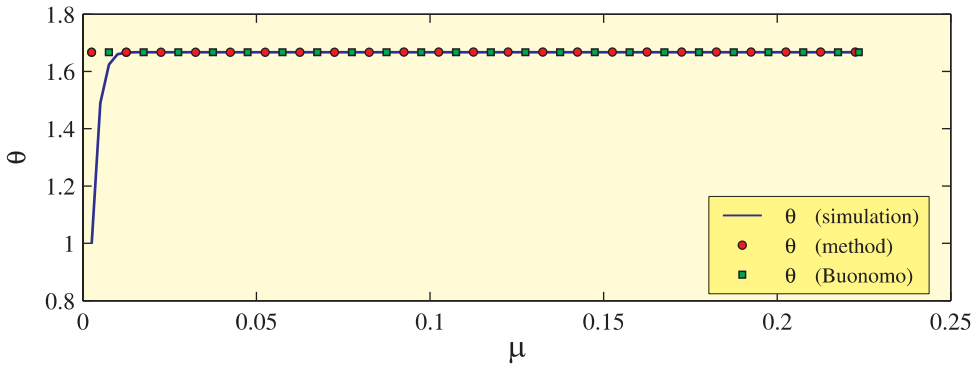

Fig. 5. Amplitude of output x_1 versus parameter μ.

Using the frequency domain method, the output is computed until the pitchfork bifurcation of the cycles is obtained with a high accuracy. Before the pitchfork bifurcation, Fig. 6(a) shows the amplitude spectrum obtained by the FFT at $\mu = 0.2$, and Fig. 6(b) depicts the similar one obtained by the proposed method. With the FFT, it is possible to obtain the spectrum after the pitchfork bifurcation, as shown in Fig. 6(c) for $\mu = 0.225$. The harmonics obtained at modes 2, 4, 6 are due to the appearance of the new stable limit cycles (they are symmetric) after the pitchfork bifurcation of cycles, but they cannot be recovered by our method, which shows a limitation of the proposed methodology.

3.2. *Chua's circuit*

Chua's circuit is an appropriate prototype for exemplifying various phenomena of complex dynamics, from the appearance of oscillations to the creation of bifurcations and chaotic attractors. In contrast to the Lorenz system that involves nonlinear functions in two variables, Chua's circuit has only one nonlinear term in a single variable. It is also proved that the generalized version of Chua's circuit has dynamic phenomena that include the route to chaos through the cascade of period-doubling process as well as to the breaking of a torus.

Chua's circuit is modeled by

$$\begin{cases} \dot{x} = \mu(y - \varphi(x)), \\ \dot{y} = x - y + z, \\ \dot{z} = -\beta y. \end{cases} \tag{15}$$

After changing coordinates $x \to x_1$, $y \to x_3$, $z \to -x_2$ to simplify the structure of the linear part, system (15) is recast as

$$\begin{cases} \dot{x}_1 = \mu(x_3 - \varphi(x_1)), \\ \dot{x}_2 = \beta x_3, \\ \dot{x}_3 = x_1 - x_2 - x_3, \end{cases} \tag{16}$$

where μ and β are control parameters, both real and positive, and $\varphi(\cdot)$ is a nonlinear function. In the electronic implementation, $\varphi(\cdot)$ is a piecewise linear function. We replace $\varphi(\cdot)$ by a cubic polynomial proposed by Khibnik *et al.* [1993]:

$$\varphi(x_1) = c_1 x_1^3 + c_2 x_1^2 + c_3 x_1 + c_4,$$

where $c_1 = 1/16$, $c_2 = 0$, $c_3 = -1/6$, $c_4 = 0$. In this setting, the dynamic behavior of the circuit looks quite similar to the original one (with a piecewise linear function).

As in Colpitts' circuit, an SISO realization is first obtained since the nonlinearity depends only on the state variable x_1. The feedback realization is

$$\mathbf{A} = \begin{bmatrix} -\dfrac{\mu c_3}{2} & 0 & \mu \\ 0 & 0 & \beta \\ 1 & -1 & -1 \end{bmatrix}, \quad \mathbf{B} = \begin{bmatrix} 1 \\ 0 \\ 0 \end{bmatrix},$$

$$\mathbf{C} = \begin{bmatrix} 1 & 0 & 0 \end{bmatrix}, \quad D = 0,$$

$$g(x) = -\mu \frac{c_3}{2} x_1 - \mu c_1 x_1^3.$$

The transfer function is

$$G(s;\mu) = \frac{2\left(s^2 + s + \beta\right)}{\Delta(s)},$$

where $\Delta(s) = 2s^3 + (2 + \mu c_3)s^2 + (2\beta + \mu c_3 - 2\mu)s + \mu\beta c_3$, and the feedback function is

$$f(e_1) = \mu \frac{c_3}{2} e_1 + \mu c_1 e_1^3.$$

The equilibrium points (output) are given by $P^0 = \hat{e}_1^0 = 0$, $P^{\pm} = \hat{e}_1^{\pm} = \pm\sqrt{-c_3/c_1}$.

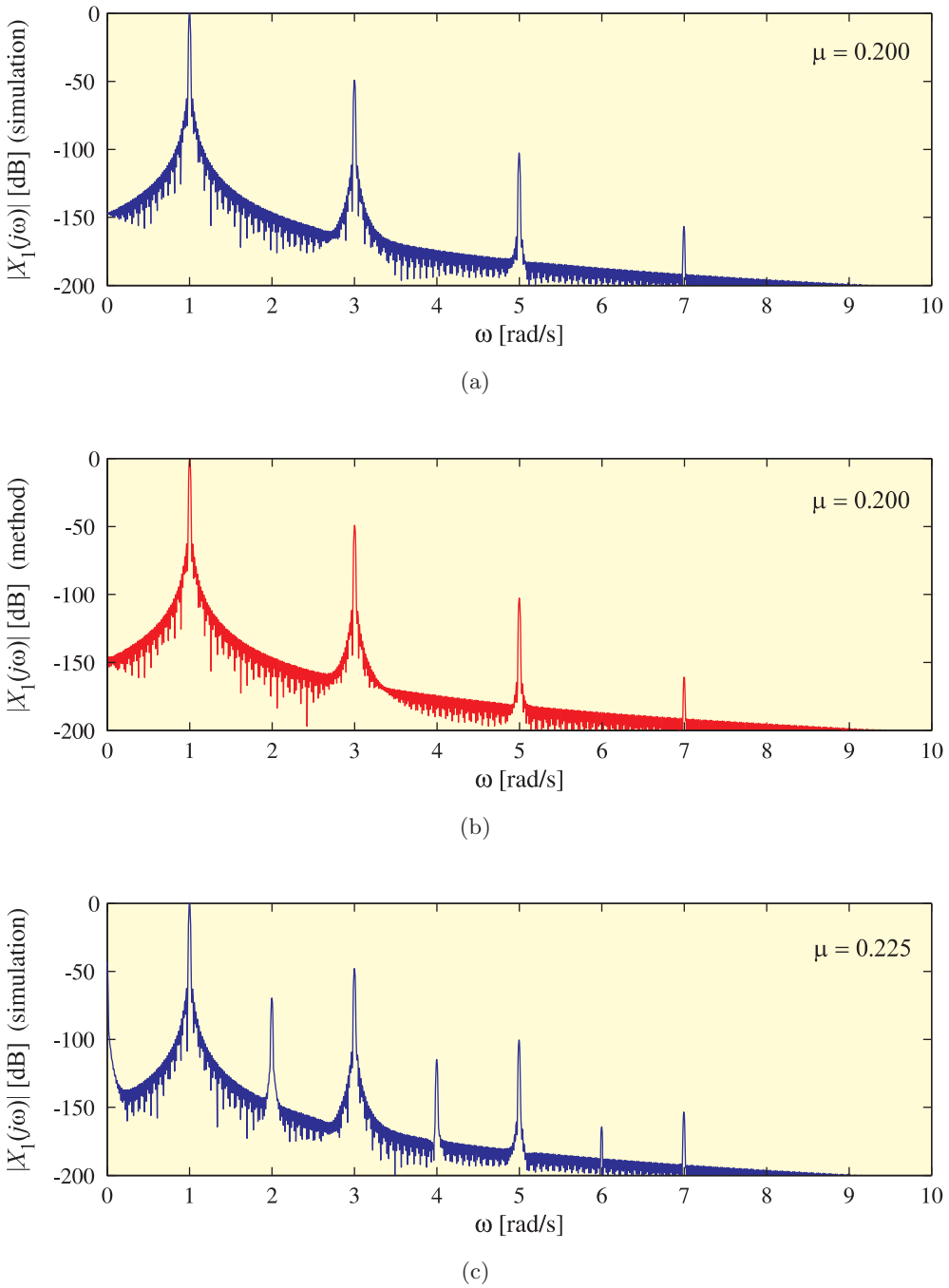

Fig. 6. Spectra of x_1 for $c_3 = -2.4$. (a) FFT method, $\mu = 0.2$. (b) Frequency method, $\mu = 0.2$. (c) FFT method (after pitchfork bifurcation), $\mu = 0.225$.

In order to study the Hopf bifurcation, the equilibrium point P^+ is considered in the following. The corresponding eigenlocus is given by

$$\hat{\lambda}(s) = G(s)J = \frac{-5\mu c_3\left(s^2 + s + \beta\right)}{\Delta(s)},$$

where $J = \mu c_3/2 + 3\mu c_1 \hat{e}_1^2\big|_{P^+} = -(5/2)\mu c_3$.

For the Hopf bifurcation ($\omega \neq 0$), the necessary condition $\hat{\lambda} = -1 + i0$ requires that ω_0 satisfies

$$\omega_0^2 = -2\mu^2 c_3(1 + 2c_3).$$

The right and left eigenvectors result in $v = w^\top = 1$, and the closed-loop transfer function is

$$H(s) = \frac{(s^2 + s + \beta)}{\Delta_1(s)},$$

where $\Delta_1(s) = s^3 + (1 - 2\mu c_3)s^2 + (\beta - 2\mu c_3 - \mu)s - 2\mu\beta c_3$.

By varying the parameters β and μ and using the frequency domain method, a period-doubling (PD) bifurcation curve is detected. In the particular case where $\beta = 9.00$, the Hopf condition is obtained for $\mu_0 = 5.083$ and the period-doubling bifurcation occurs at $\mu_{\text{PD}} = 6.011684$. With the proposed method and an eighth-order harmonic balance approximation, this value is obtained as $\mu_{\text{PD}\mathbf{M}_4} = 6.0161719$. The multipliers of the approximate monodromy matrix $\mathbf{M}_4$ are obtained as

$$\lambda_1 = 1.005827242,$$
$$\lambda_2 = -0.9995279563,$$
$$\lambda_3 = -0.1414704283 \times 10^{-2}.$$

As mentioned before, one of the multipliers must be +1.000, since it is a requirement for the technical construction of the Poincaré section. In this case, the error of the approximation of $\mathbf{M}_4$ is seen proportional to $e_{\mathbf{M}_4} = 5.827 \times 10^{-3}$.

Figure 7 shows the cycle and the frequency spectrum of the system before the PD bifurcation.

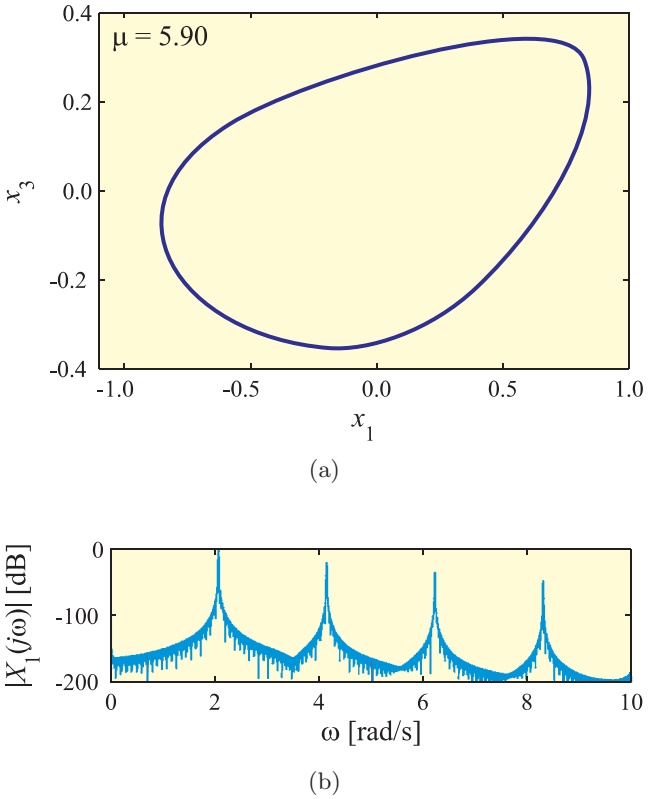

Fig. 7. (a) Limit cycle, and (b) frequency spectrum before PD bifurcation at $\mu = 5.50$.

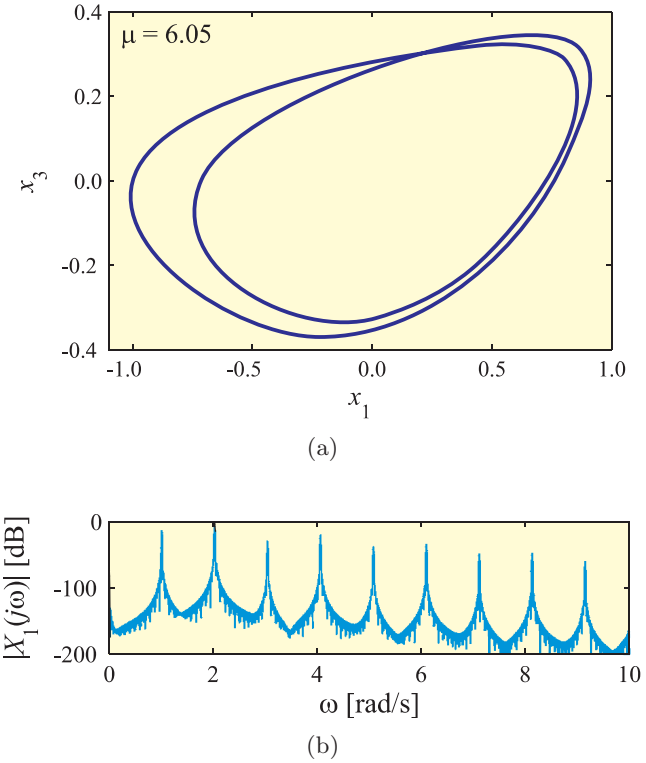

Fig. 8. (a) Limit cycle of period 2, and (b) frequency spectrum after the PD bifurcation at $\mu = 6.05$.

In this region, the frequency method is capable of determining the cycle and its power spectrum with high accuracy, which compares favorably with the FFT method.

After the PD bifurcation ($\mu = 6.05$), the cycle and the spectrum are depicted, as shown in Fig. 8, but now using only the FFT method. The spectrum shows new frequencies or modes required for a period-2 cycle. This cycle cannot be well approximated by the frequency domain method, due to the new harmonic contents and the local validity of the approximation through the Hopf bifurcation.

In order to study the harmonic distortion present in the region of period-1 cycles, comparisons of the power spectra for two values of the parameter μ were made, one near the Hopf condition ($\mu = 5.1$) and the other close to the period-doubling condition ($\mu = 6$). The oscillation frequency and the harmonics amplitude obtained with the method are compared with the ones calculated by using the FFT on the output signal obtained by simulation. The fundamental frequency of oscillation obtained with the proposed method and the one detected by the FFT are indistinguishable (Fig. 9); for that reason the power spectrum is shown versus the number of

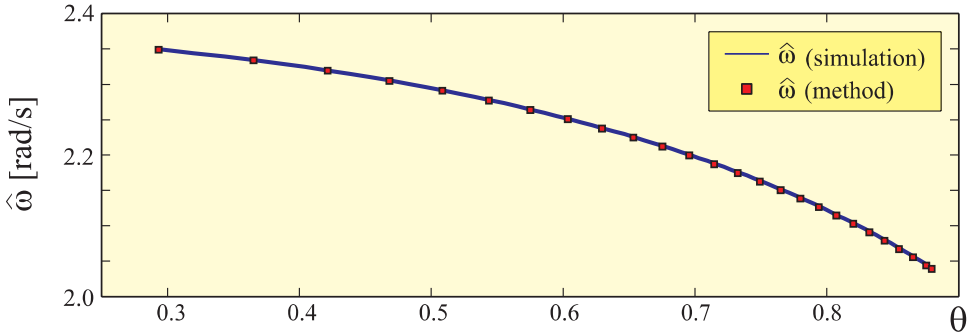

Fig. 9. Variation of the fundamental frequency versus the amplitude θ.

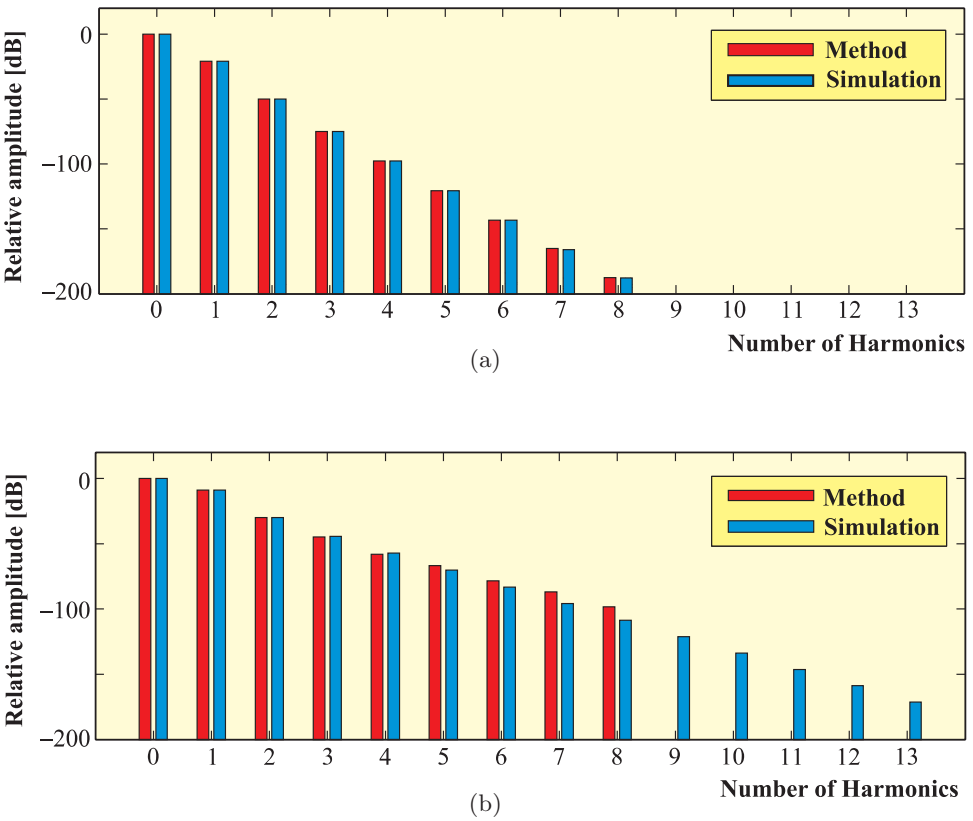

Fig. 10. Power spectrum of x_1 for $\beta = 9$. (a) $\mu = 5.1$ (close to Hopf bifurcation); (b) $\mu = 6.0$ (before the period-doubling bifurcation).

harmonics. Figure 10(a) shows that for $\mu = 5.1$ the amplitude of the harmonics obtained with the FFT is practically the same as the one obtained with the proposed eighth-order approximation; in this case the error of approximation of the Floquet multiplier is $e_{\mathbf{M}_4} = 1.12 \times 10^{-7}$. In Fig. 10(b) the amplitudes of the harmonics are observed when $\mu = 6$ by noticing the differences in the amplitudes beyond the fourth harmonic. The error of the approach grows to $e_{\mathbf{M}_4} = 5.52 \times 10^{-3}$. These results reveal that the proposed approach is very good in the neighborhood of the Hopf bifurcation, when the limit cycles are of small amplitude, and the harmonic distortions are low.

Finally, for $5.1 \leq \mu \leq 6.0$, the harmonic distortion indexes HD_2 and HD_3 are calculated in terms of the amplitude θ and compared with the ones obtained by using the FFT. These results are shown

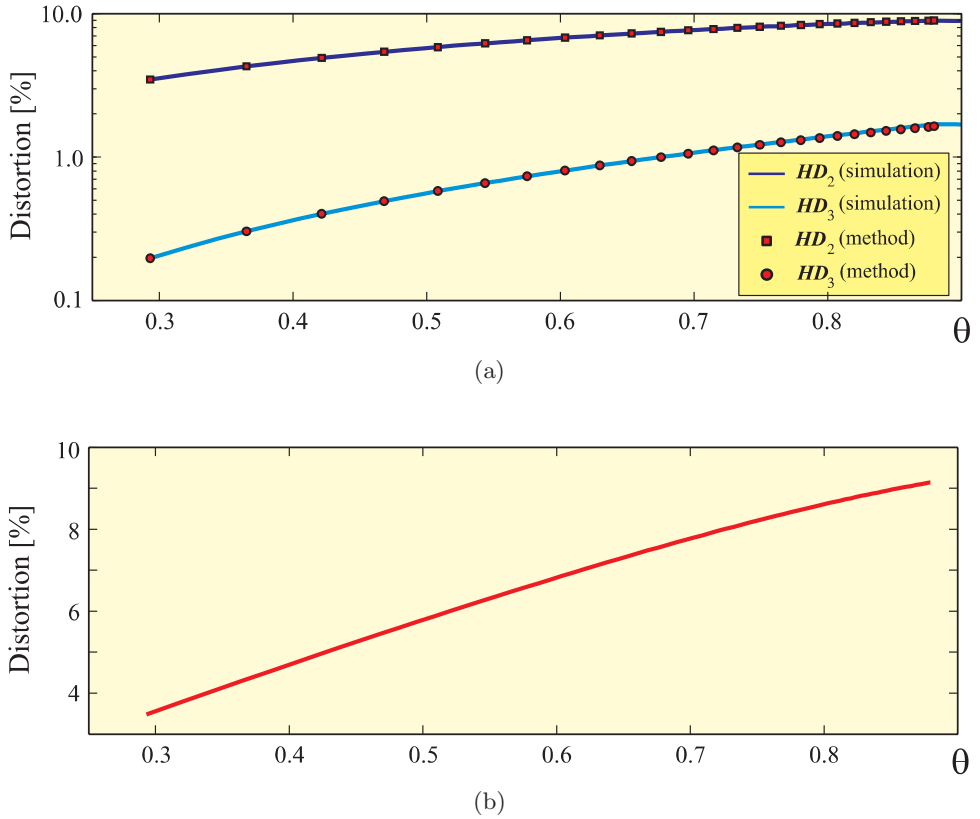

Fig. 11. Harmonic distortion of x_1 for $\beta = 9$. (a) Harmonic distortion indexes HD_2 and HD_3. (b) Total harmonic distortion (THD) by using the proposed method.

in Fig. 11(a), in which good concordance between both techniques can be observed. In Fig. 11(b), the total harmonic distortion index (THD) is shown for the same variation of μ by using the proposed approach.

4. Conclusions

It was seen that the frequency domain method is capable of estimating the oscillatory branch starting from Hopf bifurcation as well as the first bifurcation of cycles in its vicinity. The harmonic contents can be well estimated, which agree with the results obtained from a completely different approach such as using the FFT, for the primary branch of a periodic solution. The proposed method cannot handle the secondary branch of periodic solutions, such as the pitchfork, saddle-node, and period-doubling bifurcations, for which a further modification of the approach will be needed (see, for instance, [Itovich & Moiola, 2006]). In this regard, the main obstacle is the large number of harmonics involved in the secondary bifurcations, which increases the computational complexity in determining the harmonic contents.

Acknowledgments

F. I. Robbio, E. E. Paolini and J. L. Moiola appreciate the financial assistance of SGCyT-UNS and the ANPCyT (PICT-2002-11-12524). F. I. Robbio also acknowledges the financial support and the hospitality of the City University of Hong Kong. G. Chen acknowledges the financial support of City University of Hong Kong (SRG 7002134).

References

Atherton, D. P. [1975] *Nonlinear Control Engineering* (Van Nostrand Reinhold, London).

Basso, M., Genesio, R. & Tesi, A. [1997] "A frequency method for predicting limit cycle bifurcations," *Nonlin. Dyn.* **13**, 339–360.

Berns, D. W., Moiola, J. L. & Chen, G. [2001] "Detecting period-doubling bifurcation: An approximate monodromy matrix approach," *Automatica* **37**, 1787–1795.

Bonani, A. & Gilli, M. [1999] "Analysis of stability and bifurcations of limit cycles in Chua's circuit through the harmonic balance approach," *IEEE Trans. Circuits Syst.-I: Fund. Th. Appl.* **46**, 881–890.

Buonomo, A. & Di Bello, C. [1996] "Asymptotic formulas in nearly sinusoidal nonlinear oscillators," *IEEE Trans. Circuits Syst.-I*: *Fund. Th. Appl.* **43**, 953–963.

Buonomo, A. [1998a] "On the periodic solution of the van der Pol equation for small values of the damping parameter," *Int. J. Circuit Th. Appl.* **26**, 39–52.

Buonomo, A. [1998b] "The periodic solution of van der Pol's equation," *SIAM J. Appl. Math.* **59**, 156–171.

Genesio, R. & Tesi, A. [1992] "A harmonic balance approach for chaos prediction: Chua's circuit," *Int. J. Bifurcation and Chaos* **2**, 61–79.

Guckenheimer, J. & Meloon, B. [2000] "Computing periodic orbits and their bifurcations with automatic differentiation," *SIAM J. Sci. Comput.* **22**, 951–985.

Itovich, G. R. & Moiola, J. L. [2006] "On period doubling bifurcations of cycles and the harmonic balance method," *Chaos Solit. Fract.* **27**, 647–665.

Jordan, S. H. & Smith, P. [1994] *Nonlinear Ordinary Differential Equations* (Oxford University Press, Oxford).

Khibnik, A., Roose, D. & Chua, L. O. [1993] "On periodic orbits and homoclinic bifurcations in Chua's circuit with a smooth nonlinearity," *Int. J. Bifurcation and Chaos* **3**, 368–384.

Maggio, G. M., De Feo, O. & Kennedy, M. P. [1999] "Nonlinear analysis of the Colpitts oscillator and applications to design," *IEEE Trans. Circuits Syst.-I*: *Fund. Th. Appl.* **46**, 1118–1130.

Maggio, G. M., De Feo, O. & Kennedy, M. P. [2004] "A general method to predict the amplitude of oscillation in nearly sinusoidal oscillator," *IEEE Trans. Circuits Syst.-I*: *Fund. Th. Appl.* **51**, 1586–1595.

Mees, A. I. & Chua, L. O. [1979] "The Hopf bifurcation theorem and its applications to nonlinear oscillations in circuits and systems," *IEEE Trans. Circuits Syst.* **26**, 235–254.

Mees, A. I. [1981] *Dynamics of Feedback Systems* (John Wiley, Chichester).

Moiola, J. L. & Chen, G. [1996] *Hopf Bifurcation Analysis*: *A Frequency Domain Approach* (World Scientific, Singapore).

Padín, M. S., Robbio, F. I., Moiola, J. L. & Chen, G. [2005] "On limit cycle approximations in the van der Pol oscillator," *Chaos Solit. Fract.* **23**, 207–220.

Piccardi, C. [1994] "Bifurcations of limit cycles in periodically forced nonlinear systems: The harmonic balance approach," *IEEE Trans. Circuits Syst.-I*: *Fund. Th. Appl.* **41**, 315–320.

Piccardi, C. [1996] "Harmonic balance analysis of codimension 2 bifurcations in periodic systems," *IEEE Trans. Circuits Syst.-I*: *Fund. Th. Appl.* **43**, 1015–1018.

Qiu, S. S. & Filanovsky, I. M. [1987] "Periodic solutions of the van der Pol equation with moderate values of damping coefficient," *IEEE Trans. Circuits Syst.* **34**, 913–918.

Robbio, F. I., Alonso, D. M. & Moiola, J. L. [2004a] "Detection of limit cycle bifurcations using harmonic balance methods," *Int. J. Bifurcation and Chaos* **10**, 3647–3654.

Robbio, F. I., Padín, M. S., Moiola, J. L. & Chen, G. [2004b] "Computation of sinusoidal regime in the Colpitts oscillator," *Dyn. Cont. Discr. Impul. Syst.*, *Series B*: *Appl. Algorith.* **11a**, 144–151.

Sansen, W. [1999] "Distortion in elementary transistor circuits," *IEEE Trans. Circuits Syst.-II*: *Anal. Dig. Sign. Proc.* **46**, 315–325.

Strogatz, S. H. [1994] *Nonlinear Dynamics and Chaos — With Applications to Physics*, *Biology*, *Chemistry and Engineering* (Addison-Wesley, Reading).

Torrini, G., Genesio, R. & Tesi, A. [1998] "On the computation of characteristic multipliers for predicting limit cycle bifurcations," *Chaos Solit. Fract.* **9**, 121–133.